Cascaded TAS/MRC in MIMO Multiuser Relay Networks

Nan Yang, *Member, IEEE,* Phee Lep Yeoh, *Member, IEEE,* Maged Elkashlan, *Member, IEEE,* Jinhong Yuan, *Senior Member, IEEE,* and Iain B. Collings, *Senior Member, IEEE*

***Abstract*—We propose cascaded transmit antenna selection with maximal-ratio combining (TAS/MRC) for use in multiuser relay networks (MRN) with N_S, N_R, and N_D antennas at the source, the relay, and each of the K destinations, respectively. We consider opportunistic scheduling where the destination with the highest instantaneous end-to-end signal-to-noise ratio (SNR) is scheduled for transmission. In cascaded TAS/MRC, a single transmit antenna that maximizes the instantaneous received SNR in each hop is selected, and all the receive antennas are MRC combined. We derive new exact closed-form statistics of the end-to-end SNR, from which we derive the exact and the approximate symbol error rate (SER) for M-ary quadrature amplitude modulation (M-QAM) and M-ary phase-shift keying (M-PSK). New concise expressions are derived to characterize the diversity order and the array gain. We highlight that our proposed scheme attains the maximum diversity order of $N_R \times \min\{N_S, N_D K\}$. Furthermore, we determine the optimal power assignment at the source and the relay that minimizes the SER.**

***Index Terms*—MIMO, multiuser, power assignment, relays.**

I. Introduction

In multiuser networks, the deployment of cooperative relays between the wireless access point and the user terminals is a promising solution to increase the transmission rate and extend network coverage [1, 2]. This network architecture, referred to as multiuser relay networks (MRN), is well-suited to emerging technologies such as IEEE 802.16j mobile multihop relay (MMR) [3] and IEEE 802.11s mesh networks [4]. Driven by these, MRN with single antenna nodes has been analyzed in several recent contributions [5–8].

Manuscript received February 18, 2011; revised August 30, 2011 and June 25, 2012; accepted June 28, 2012. The associate editor coordinating the review of this paper and approving it for publication was S. D. Blostein.

This work was supported in part by a CSIRO OCE postdoctoral fellowship, and in part by the Australian Research Council Discovery Project DP120102607. Part of this work was presented at the IEEE Global Telecommunication Conference, Houston, Texas, USA, 2011.

N. Yang and I. B. Collings are with the Wireless and Networking Technologies Laboratory, CSIRO ICT Centre, Marsfield, NSW 2122, Australia (e-mail: {jonas.yang, iain.collings}@csiro.au).

P. L. Yeoh is with the Department of Electrical and Electronic Engineering, University of Melbourne, Parkville, VIC 3010, Australia (e-mail: phee.yeoh@unimelb.edu.au).

M. Elkashlan is with the School of Electronic Engineering and Computer Science, Queen Mary, University of London, London E1 4NS, UK (e-mail: maged.elkashlan@eecs.qmul.ac.uk).

J. Yuan is with the School of Electrical Engineering and Telecommunications, University of New South Wales, Sydney, NSW 2052, Australia, and also with the Wireless and Networking Technologies Laboratory, CSIRO ICT Centre, Marsfield, NSW 2122, Australia (e-mail: j.yuan@unsw.edu.au).

Digital Object Identifier 10.1109/TWC.2012.081312.120866

The principal challenge in MRN is to achieve low error rates in a manner which requires low-complexity processing and reduced feedback overhead. A prospective solution is to install multiple antennas at all the nodes to exploit the benefits of multiple-input multiple-output (MIMO) transmission. MIMO is well-known to achieve transmit/receive diversities and boost the link reliability [9–11]. Against this background, we focus our attention on MIMO transmission in MRN to guarantee high data rates over wide areas. Foundational work on MIMO MRN has concentrated on the capacity and/or throughput performance from an information theoretic perspective. The key results in [12] include upper and lower bounds on the achievable sum rate for fixed relays with linear operations. In [13], the sum rate was further analyzed for both half-duplex and full-duplex relays. The maximization of the network throughput under a power constraint was investigated in [14]. In [15], the joint optimization of linear beamforming and power control was addressed with the objective of minimizing the power consumption at the source and the relay.

In this paper, we propose transmit antenna selection with maximal-ratio combining (TAS/MRC) as a solution to the problem of achieving high performance in MIMO MRN with low computational complexity and low feedback overhead. In point-to-point MIMO communications and dual-hop MIMO relaying, TAS/MRC is a proven cost-conscious strategy to achieve full transmit and receive diversity [16–18]. With this strategy, a single transmit antenna that maximizes the post-processed signal-to-noise ratio (SNR) at the receiver is selected, and all the receive antennas are combined with MRC. In doing so, only the index of the selected antenna is fed back to the transmitter. As such, our scheme significantly reduces the feedback overhead compared with beamforming (e.g., [12] and [15]) which requires the feedback of the channel estimates for all the antennas. Furthermore, TAS/MRC enables the transmitter to be easily implemented with a single radio frequency (RF) chain and an analog switch [19], whereas beamforming requires multiple RF chains. Therefore, our scheme is well-suited for network nodes that are subject to resource constraints such as a single transmit chain and a single-chip implementation.

We consider MIMO MRN with N_S, N_R, and N_D antennas at the source, the relay, and each of the K destinations, respectively. Among the K destinations, a single destination with the highest instantaneous end-to-end SNR is scheduled for transmission. For this network, we propose TAS/MRC in a cascaded fashion. In the first hop, a single antenna is selected

1536-1276/12$31.00 © 2012 IEEE

at the source while all the antennas at the relay are MRC combined. In the second hop, a single antenna is selected at the relay while all the antennas at the scheduled destination are MRC combined. We take into account amplify-and-forward (AaF) relaying as a practical relay implementation which offers short signal processing delays without any decoding and re-encoding operations at the relay.

The primary contributions of this paper are summarized as follows:

1) We provide important quality of service measures by deriving new exact closed-form expressions for the cumulative distribution function (CDF) and the moment generating function (MGF), which are valid for the practical assumption of unbalanced Rayleigh fading between the hops.
2) We derive new first-order expansions for the CDF and the MGF, which are valuable in providing further insights into the joint effects of antenna configuration and number of destinations on the network performance.
3) We derive a new accurate approximation for the symbol error rate (SER) with M-ary quadrature amplitude modulation (M-QAM) which is directly in terms of the MGF expression. Our approximation is given in closed-form, which avoids cumbersome numerical integration.
4) To obtain further insights, we derive new closed-form expressions for the asymptotic SER with M-QAM and M-ary phase-shift keying (M-PSK). Our asymptotic solutions identify the diversity order and the array gain; two distinctive parameters that govern the SER in the high SNR regime.
5) Based on our approximate and asymptotic SER solutions, we determine the optimal power assignment at the source and the relay aimed at minimizing the SER under a total power constraint in the network.

Our new analytical expressions apply to general operating scenarios with arbitrary number of antennas N_S, N_R, and N_D, arbitrary number of destinations K, and distinct average received SNRs between the hops. Our asymptotic solutions evidently demonstrate that cascaded TAS/MRC with opportunistic scheduling achieves the maximum diversity order of $N_R \times \min\{N_S, N_D K\}$. We further show that our proposed power assignment strategy yields a superior performance compared to uniform power assignment.

Notation: Scalar variables are denoted by italic symbols. Vectors and matrices are denoted by lower-case and upper-case boldface symbols, respectively. Given a complex vector $\mathbf{x}$, $\|\mathbf{x}\|$ denotes the Euclidean norm and $(\mathbf{x})^\dagger$ denotes the conjugate transpose. The $m \times m$ identity matrix is referred to as $\mathbf{I}_m$. The expectation is denoted by $\mathbb{E}[\cdot]$.

II. MIMO MRN WITH CASCADED TAS/MRC

Fig. 1 depicts a MIMO MRN where the relay, equipped with N_R antennas, assists the communication between the source, equipped with N_S antennas, and the K destinations, each equipped with N_D antennas. Note that the direct links between the source and the destinations are in absence which is common in scenarios where the destinations are located far away from the source or within heavily shadowed areas. The

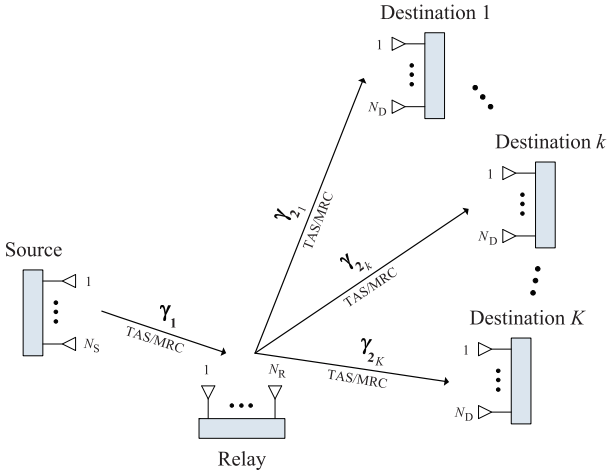

Fig. 1. MIMO MRN with N_S, N_R, and N_D antennas at the source, relay, and destination, respectively. In each hop, only one transmit antenna is selected for transmission while all the receive antennas are MRC combined.

antennas at each terminal are sufficiently spaced apart such that the links between the transmit and receive antenna pairs are uncorrelated.

The transmission is facilitated on a time-frame basis where the channel state information (CSI) of all the terminals is constant within each frame but varies from one frame to another. In each link, we assume that CSI is estimated by the receiver using pilot symbols sent by the transmitter prior to data transmission. In the source-relay link, the source transmits pilot symbols and the relay feeds back the index of the best transmit antenna to the source. In the relay-destination link, the relay broadcasts pilot symbols and each destination feeds back the index of the best transmit antenna and the corresponding channel estimates to the relay.

In this network, the principle of opportunistic scheduling [20] is adopted to prioritize the transmission of individual messages to multiple destinations. Under this principle, the instantaneous end-to-end SNR associated with the scheduled destination is defined as

$$\gamma_s = \max_{1 \le k \le K} \{\gamma_{r_k}\}, \tag{1}$$

where γ_{r_k} is the instantaneous end-to-end SNR of the kth destination. Opportunistic scheduling has been adopted in a number of downlink multiuser networks, such as high-speed downlink packet access [21] and evolution-data optimized [22], to profit from multiuser diversity.

We proceed to detail the cascaded TAS/MRC in MIMO MRN, as follows:

1) Source-to-relay TAS/MRC. In the first hop, the source transmits a scalar symbol x to the relay with zero mean and unit variance. We denote $\mathbf{h}_{i,\mathrm{R}}$ as the $N_R \times 1$ Rayleigh channel vector between the i-th transmit antenna at the source and the N_R receive antennas at the relay. As such, the received signal at the relay is written as

$$\mathbf{y}_{\mathrm{SR}} = \sqrt{E_{\mathrm{S}}}\mathbf{h}_{\mathrm{SR}} x + \mathbf{n}_{\mathrm{SR}}, \tag{2}$$

where

$$\|\mathbf{h}_{\mathrm{SR}}\| = \max_{1 \le i \le N_S} \{\|\mathbf{h}_{i,\mathrm{R}}\|\} \tag{3}$$

is the largest channel vector norm between the source and the relay, $E_{\rm S}$ is the available transmit power at the source, and $\mathbf{n}_{\rm SR}$ is the $N_R \times 1$ additive white Gaussian noise (AWGN) satisfying $\mathbb{E}\left[\mathbf{n}_{\rm SR}\mathbf{n}_{\rm SR}^{\dagger}\right] = \mathbf{I}_{N_R}\Omega$, where Ω is the one-sided power spectral density (PSD) of the noise at each receive antenna. The relay combines the received signal vector in (2) using MRC to form a single scalar symbol x^* given by

$$x^* = \mathbf{h}_{\rm SR}^{\dagger}\mathbf{y}_{\rm SR} = \sqrt{E_{\rm S}}\mathbf{h}_{\rm SR}^{\dagger}\mathbf{h}_{\rm SR}x + \mathbf{h}_{\rm SR}^{\dagger}\mathbf{n}_{\rm SR}. \tag{4}$$

2) Relay-to-destination TAS/MRC. In the second hop, the relay applies a scaling gain G to x^* and forwards the scaled signal to the destination with the highest instantaneous end-to-end SNR. We denote $\mathbf{g}_{j,{\rm D}_k}$ as the $N_D \times 1$ Rayleigh channel vector between the j-th transmit antenna at the relay and the N_D receive antennas at the k-th destination. As such, the received signal vector at the k-th destination is expressed as

$$\mathbf{y}_{{\rm RD}_k} = \sqrt{E_{\rm R}}\mathbf{g}_{{\rm RD}_k}G\left(\sqrt{E_{\rm S}}\mathbf{h}_{\rm SR}^{\dagger}\mathbf{h}_{\rm SR}x + \mathbf{h}_{\rm SR}^{\dagger}\mathbf{n}_{\rm SR}\right) + \mathbf{n}_{{\rm RD}_k}, \tag{5}$$

where

$$\|\mathbf{g}_{{\rm RD}_k}\| = \max_{1\le j\le N_R}\{\|\mathbf{g}_{j,{\rm D}_k}\|\} \tag{6}$$

is the largest channel vector norm between the relay and the k-th destination, $E_{\rm R}$ is the available transmit power at the relay, and $\mathbf{n}_{{\rm RD}_k}$ is the $N_D \times 1$ AWGN vector satisfying $\mathbb{E}\left[\mathbf{n}_{{\rm RD}_k}\mathbf{n}_{{\rm RD}_k}^{\dagger}\right] = \mathbf{I}_{N_D}\Omega$. The destination combines the received signal vector using MRC. Therefore, the instantaneous end-to-end SNR of the k-th destination is given by

$$\gamma_{r_k} = \frac{\gamma_1\gamma_{2_k}}{\gamma_{2_k} + \frac{1}{\|\mathbf{h}_{\rm SR}\|^2G^2\Omega}}, \tag{7}$$

where $\gamma_1 = \|\mathbf{h}_{\rm SR}\|^2E_{\rm S}/\Omega$ and $\gamma_{2_k} = \|\mathbf{g}_{{\rm RD}_k}\|^2E_{\rm R}/\Omega$ represent the instantaneous SNRs of the first and second hops, respectively. Correspondingly, the average SNRs of the first and second hops are given by $\overline{\gamma}_1 = \mathbb{E}[\gamma_1]$ and $\overline{\gamma}_{2_k} = \mathbb{E}[\gamma_{2_k}]$, respectively. We assume that the destinations are located in a homogeneous environment with the same average SNR of the second hop such that $\overline{\gamma}_{2_k} = \overline{\gamma}_2\ \forall\ k$. In practice, this applies to the scenario where the destinations are located in a cluster (e.g., office building). In such a scenario, the destinations are relatively close together but far off from the relay. Of course, we retain the practical consideration of unbalanced hops where $\overline{\gamma}_1 \neq \overline{\gamma}_2$, which is typical of relaying applications where the signals transmitted in the first and the second hops experience different radio environments.

It is evident from (7) that the choice of the scaling gain G determines the instantaneous end-to-end SNR. We focus our attention on variable gain AaF relaying [23], where the knowledge of the source-relay link fading coefficients is utilized to invert the channel in the first hop. Under this relaying protocol, the scaling gain G is defined as

$$G = \frac{1}{\sqrt{E_S\|\mathbf{h}_{\rm SR}\|^4 + \xi\Omega\|\mathbf{h}_{\rm SR}\|^2}}, \tag{8}$$

where $\|\mathbf{h}_{\rm SR}\|$ is defined in (3). In (8), we consider two relaying protocols: the channel-noise-based (CNB) relaying with $\xi = 1$ and the channel-based (CB) relaying with $\xi = 0$. CNB relaying accounts for the noise variance at the relay and thus limits the output power of the relay when $\|\mathbf{h}_{\rm SR}\|^2$ is low. CB relaying does not account for the noise variance at the relay and thus has the effect of inverting the channel in the first hop. We note that CB relaying asymptotically approaches CNB relaying at high SNR. Inserting (8) into (7), the instantaneous end-to-end SNR of the k-th destination is given by

$$\gamma_{r_k} = \frac{\gamma_1\gamma_{2_k}}{\gamma_1 + \gamma_{2_k} + \xi}. \tag{9}$$

Finally, according to (1), the destination with the highest γ_{r_k} is scheduled for transmission.

III. New Statistical Properties of the Instantaneous End-to-End SNR

A. New Exact Results

In this subsection, we present new exact closed-form expressions for the CDF and the MGF of the instantaneous end-to-end SNR, γ_s, which allow for arbitrary numbers of antennas and destinations. These results will be used to derive the exact and approximate SER.

Theorem 1: The CDF of γ_s is derived as (10) on the top of the next page, which is valid for unbalanced fading between the hops. In (10), $\psi_v = \sum_{v=1}^{N_D-1} j_v$ with $j_0 = \kappa$ and $j_{N_D} = 0$, $\psi_w = \sum_{w=1}^{N_R-1} k_w$ with $k_0 = \lambda$ and $k_{N_R} = 0$, $\nu = N_R - \epsilon - \alpha + \psi_w - \beta$, and $K_v(\cdot)$ is the vth-order modified Bessel function of the second kind.

Proof: See Appendix A. ∎

It is worth noting that (10) involves only finite summations of exponentials, powers, and Bessel functions, thus can be calculated in closed-form. The outage probability is obtained directly from (10) according to

$$P_{\rm out} = F_{\gamma_s}(\gamma_{\rm th}), \tag{11}$$

where $P_{\rm out}$ is the probability that γ_s drops below a predetermined threshold SNR $\gamma_{\rm th}$.

To evaluate the MGF of γ_s, $M_{\gamma_s}(s)$, we use the derivative property of the Laplace transform to express $M_{\gamma_s}(s)$ in terms of $f_{\gamma_s}(\gamma)$ as

$$M_{\gamma_s}(s) = -s\int_0^{\infty} F_{\gamma_s}(\gamma)\, e^{s\gamma}d\gamma. \tag{12}$$

In the derivation of $M_{\gamma_s}(s)$, we find that the closed-form solution for CNB relaying with $\xi = 1$ is analytically intractable. As such, we concentrate on the analytically tractable choice of CB relaying with $\xi = 0$. This has been commonly adopted in the recent open literature, e.g., [24–26]. Based on (12), we present a new closed-form expression for $M_{\gamma_s}(s)$, as given in the following theorem.

Theorem 2: The MGF of γ_s is derived as (13) on the next page, where $\rho_1 = \psi_v + \epsilon + \alpha + \beta + 1$, $\rho_2 = 2N_R + \psi_v - \epsilon - \alpha + 2\psi_w - \beta + 1$, $\Gamma(\cdot)$ is the Gamma function, and ${}_2F_1(\cdot,\cdot;\cdot;\cdot)$ is the Gauss hypergeometric function.

Proof: By substituting (10) into (12) and using the identity [27, eq. (2.16.1.3)] to solve the resultant integral, we obtain the desired result in (13). ∎

Our result in (13) is easy to handle since it contains simple exponentials, powers, and hypergeometric functions.

$$F_{\gamma_s}(\gamma) = 1 + \frac{2N_S}{\Gamma(N_R)} \sum_{\kappa=1}^{N_R K} \binom{N_R K}{\kappa} \sum_{\lambda=0}^{N_S-1} \binom{N_S-1}{\lambda} (-1)^{\kappa+\lambda} \sum_{\epsilon=0}^{N_R-1} \binom{N_R-1}{\epsilon} \prod_{v=1}^{N_D-1} \left[\sum_{j_v=0}^{j_{v-1}} \binom{j_{v-1}}{j_v} \left(\frac{1}{v!}\right)^{j_v - j_{v+1}} \right]$$
$$\times \prod_{w=1}^{N_R-1} \left[\sum_{k_w=0}^{k_{w-1}} \binom{k_{w-1}}{k_w} \left(\frac{1}{w!}\right)^{k_w - k_{w+1}} \right] \sum_{\alpha=0}^{\psi_v} \binom{\psi_v}{\alpha} \sum_{\beta=0}^{\psi_w} \binom{\psi_w}{\beta} \left(\frac{\kappa}{\lambda+1}\right)^{\frac{\nu}{2}} \overline{\gamma}_1^{-\left(\frac{\nu}{2}+\epsilon+\alpha+\beta\right)} \overline{\gamma}_2^{-\left(\frac{\nu}{2}+\psi_v\right)}$$
$$\times \gamma^{\frac{\nu}{2}+\epsilon+\beta+\psi_v} (\gamma+\xi)^{\frac{\nu}{2}+\alpha} e^{-\gamma\left(\frac{\lambda+1}{\overline{\gamma}_1}+\frac{\kappa}{\overline{\gamma}_2}\right)} K_\nu \left(2\sqrt{\frac{\kappa(\lambda+1)\gamma(\gamma+\xi)}{\overline{\gamma}_1\overline{\gamma}_2}} \right). \quad (10)$$

$$M_{\gamma_s}(s) = 1 - \frac{N_S\sqrt{\pi}s}{\Gamma(N_R)} \sum_{\kappa=1}^{N_R K} \binom{N_R K}{\kappa} \sum_{\lambda=0}^{N_S-1} \binom{N_S-1}{\lambda} (-1)^{\kappa+\lambda} \sum_{\epsilon=0}^{N_R-1} \binom{N_R-1}{\epsilon} \prod_{v=1}^{N_D-1} \left[\sum_{j_v=0}^{j_{v-1}} \binom{j_{v-1}}{j_v} \left(\frac{1}{v!}\right)^{j_v - j_{v+1}} \right]$$
$$\times \prod_{w=1}^{N_R-1} \left[\sum_{k_w=0}^{k_{w-1}} \binom{k_{w-1}}{k_w} \left(\frac{1}{w!}\right)^{k_w - k_{w+1}} \right] \sum_{\alpha=0}^{\psi_v} \binom{\psi_v}{\alpha} \sum_{\beta=0}^{\psi_w} \binom{\psi_w}{\beta} \frac{2^{-\rho_2+1} \left(\frac{\lambda+1}{\overline{\gamma}_1} + \frac{\kappa}{\overline{\gamma}_2} - s\right)^{-\rho_1}}{(\lambda+1)^\nu \overline{\gamma}_1^{\epsilon+\alpha+\beta} \overline{\gamma}_2^{\psi_v}}$$
$$\times \frac{\Gamma(\rho_1)\Gamma(\rho_2)}{\Gamma\left(N_R+\psi_v+\psi_w+\frac{3}{2}\right)} {}_2F_1\left(\frac{\rho_1}{2}, \frac{\rho_1+1}{2}; N_R+\psi_v+\psi_w+\frac{3}{2}; 1 - \frac{4\kappa(\lambda+1)\overline{\gamma}_1\overline{\gamma}_2}{\left(\kappa\overline{\gamma}_1 + (\lambda+1)\overline{\gamma}_2 - s\overline{\gamma}_1\overline{\gamma}_2\right)^2} \right). \quad (13)$$

B. New Asymptotic Results

In this subsection, we derive new concise first order expansions for the CDF and the MGF of γ_s. Our results will allow us to examine the asymptotic SER in the high SNR regime. We note that CNB relaying exhibits the same asymptotic behavior as CB relaying [23]. As such, the asymptotic results presented in this paper are applicable to both CNB relaying and CB relaying.

Theorem 3: The first order expansions of $F_{\gamma_s}(\gamma)$ and $M_{\gamma_s}(s)$ are given by

$$F_{\gamma_s}^{\infty}(\gamma) = \left(\frac{\delta}{\overline{\gamma}_1^{\phi}}\right) \gamma^{\phi} + o\left(\gamma^{\phi}\right) \quad (14)$$

and

$$M_{\gamma_s}^{\infty}(s) = \frac{\delta\Gamma(\phi+1)}{(-s\overline{\gamma}_1)^{\phi}} + o\left(\overline{\gamma}_1^{-\phi}\right), \quad (15)$$

respectively. In (14) and (15), we define

$$\phi = N_R \times \min\{N_S, N_D K\}, \quad (16)$$

and

$$\delta = \begin{cases} \frac{1}{(N_R!)^{N_S}}, & N_S < N_D K \\ \frac{1}{(N_D!)^{N_R K} \omega^{N_R N_D K}}, & N_S > N_D K \\ \frac{1}{(N_R!)^{N_S}} + \frac{1}{(N_D!)^{N_R K} \omega^{N_R N_D K}}, & N_S = N_D K, \end{cases} \quad (17)$$

with $\omega = \overline{\gamma}_2/\overline{\gamma}_1$.

Proof: See Appendix B. ∎

These expressions illustrate the contributions from each of the individual network parameters: the number of antennas, the number of destinations, and the per-hop average SNRs.

Note that the first order expansion of $F_{\gamma_s}(\gamma)$ represents the asymptotic outage probability. As such, we see from (14) that in the low outage regime, the outage probability scales inversely with $N_R \times \min\{N_S, N_D K\}$. While the outage is limited by the minimum of N_S and $N_D K$, it is directly proportional to N_R.

IV. SER of Cascaded TAS/MRC in MIMO MRN

A. Exact and Approximate SER

The traditional approach to evaluating the SER for a variety of modulations is to average the conditional error probability, $P(e|\gamma)$, over the probability density function (PDF) of γ_s, i.e.,

$$P_s = \int_0^{\infty} P(e|\gamma) f_{\gamma_s}(\gamma) d\gamma, \quad (18)$$

where $P(e|\gamma) = aQ\left(\sqrt{2b\gamma}\right)$, with $Q(\cdot)$ denoting the Gaussian Q-function, and a and b are modulation-specific constants. The expression in (18) can be conveniently re-expressed in terms of the MGF of γ_s to derive new SER expressions under M-QAM and M-PSK modulations.

1) M-QAM: The exact SER of M-QAM can be expressed as [28]

$$P_{s,\mathrm{MQAM}} = \frac{4\Delta}{\pi} \int_0^{\frac{\pi}{2}} M_{\gamma_s}\left(-\frac{g_{\mathrm{MQAM}}}{\sin^2\theta}\right) d\theta - \frac{4\Delta^2}{\pi} \int_0^{\frac{\pi}{4}} M_{\gamma_s}\left(-\frac{g_{\mathrm{MQAM}}}{\sin^2\theta}\right) d\theta, \quad (19)$$

where $\Delta = 1 - 1/\sqrt{M}$ and $g_{\mathrm{MQAM}} = 3/2(M-1)$. Capitalizing on our new MGF expression in (13), the exact SER can be obtained by evaluating the integrals in (19) numerically. We note that seeking a closed-form solution to (19) is intractable due to the integration over θ.

We note that seeking a closed-form solution to (19) is intractable due to the integration over θ. To avoid this integration, we present a new and accurate approximation to (19). Specifically, the approximate SER of M-QAM is derived in

closed-form as

$$P_{s,\mathrm{MQAM}} \approx \frac{\Delta\left(2+\Delta\right)}{6} M_{\gamma_s}\left(-g_{\mathrm{MQAM}}\right) + \Delta\left(1-\Delta\right) M_{\gamma_s}\left(-\frac{4}{3} g_{\mathrm{MQAM}}\right) + \frac{\Delta^2}{2} M_{\gamma_s}\left(-2 g_{\mathrm{MQAM}}\right), \tag{20}$$

where $M_{\gamma_s}(\cdot)$ is given in (13). Our result applies to arbitrary numbers of antennas and destinations, which provides a computationally efficient alternative to numerical simulations. Our numerical results will demonstrate the accuracy of this approximation.

Proof: See Appendix C. ∎

2) M-PSK: For completeness, we present the exact and the approximate SER expressions for M-PSK. Utilizing the standard result in [28], we express the exact SER of M-PSK as

$$P_{s,\mathrm{MPSK}} = \frac{1}{\pi}\int_0^{\Theta} M_{\gamma_s}\left(-\frac{g_{\mathrm{MPSK}}}{\sin^2\theta}\right) d\theta, \tag{21}$$

where $\Theta = \pi\left(M-1\right)/M$ and $g_{\mathrm{MPSK}} = \sin^2\left(\pi/M\right)$. With the aid of (13), the exact SER is obtained via numerical integration. Given the intractability of an exact closed-form solution, an accurate approximation to (21) is given by [29]

$$P_{s,\mathrm{MPSK}} \approx \left(\frac{\Theta}{2\pi}-\frac{1}{6}\right) M_{\gamma_s}\left(-g_{\mathrm{MPSK}}\right) + \frac{1}{4} M_{\gamma_s}\left(-\frac{4 g_{\mathrm{MPSK}}}{3}\right) + \left(\frac{\Theta}{2\pi}-\frac{1}{4}\right) M_{\gamma_s}\left(-\frac{g_{\mathrm{MPSK}}}{\sin^2\Theta}\right). \tag{22}$$

Substituting (13) into (22) yields the desired approximate SER.

B. Asymptotic SER

In this subsection, we focus on the reliable operating condition of low SER typically in the order of $P_s \approx 10^{-4}$, which in turn corresponds to the high SNR regime. In this regime, the key factors governing network performance are the diversity order and the array gain. By applying a general parameterized result from [30], the asymptotic SER can be expressed as

$$P_s^{\infty} = \left(G_a \overline{\gamma}_1\right)^{-G_d} + o\left(\overline{\gamma}_1^{-G_d}\right), \tag{23}$$

where $o(\cdot)$ denotes the higher order terms. In (23), G_d is the diversity order, which determines the asymptotic slope of the SER curve and is given by

$$G_d = \lim_{\overline{\gamma}_1 \to \infty} -\frac{\log P_s}{\log \overline{\gamma}_1}, \tag{24}$$

while G_a is the array gain, which provides a measure of the SNR advantage of the SER curve with respect to a reference curve of $\overline{\gamma}_1^{-G_d}$.

We now proceed to derive the asymptotic SER for M-QAM and M-PSK based on $M_{\gamma_s}^{\infty}(s)$ in (15).

1) M-QAM: Substituting (15) into (19) yields

$$P_{s,\mathrm{MQAM}}^{\infty} = \frac{4\Delta\delta\Gamma\left(\phi+1\right)}{\pi\overline{\gamma}_1^{\phi}\left(g_{\mathrm{MQAM}}\right)^{\phi}} \int_0^{\frac{\pi}{2}} \left(\sin\theta\right)^{2\phi} d\theta - \frac{4\Delta^2\delta\Gamma\left(\phi+1\right)}{\pi\overline{\gamma}_1^{\phi}\left(g_{\mathrm{MQAM}}\right)^{\phi}} \int_0^{\frac{\pi}{4}} \left(\sin\theta\right)^{2\phi} d\theta. \tag{25}$$

Rearranging the integration limits and solving the resultant integrals in (25), we obtain a new closed-form expression for the asymptotic SER of M-QAM which is given by

$$P_{s,\mathrm{MQAM}}^{\infty} = \left(G_{a,\mathrm{MQAM}}\overline{\gamma}_1\right)^{-G_{d,\mathrm{MQAM}}} + o\left(\overline{\gamma}_1^{-G_{d,\mathrm{MQAM}}}\right). \tag{26}$$

where the diversity order is

$$G_{d,\mathrm{MQAM}} = N_R \times \min\{N_S, N_D K\} \tag{27}$$

and the array gain is

$$G_{a,\mathrm{MQAM}} = \left[\frac{2\Delta\left(1-\Delta\right)\delta\Gamma\left(\phi+\frac{1}{2}\right)}{\sqrt{\pi}\left(g_{\mathrm{MQAM}}\right)^{\phi}} + \frac{4\Delta^2\delta\Gamma\left(\phi+1\right)}{\pi\left(g_{\mathrm{MQAM}}\right)^{\phi}} \times {}_2F_1\left(\frac{1}{2}, 1+\phi; \frac{3}{2}; -1\right)\right]^{-\frac{1}{\phi}}, \tag{28}$$

with ϕ and δ defined in (16) and (17), respectively.

2) M-PSK: Substituting (15) into (21) results in

$$P_{s,\mathrm{MPSK}}^{\infty} = \frac{\delta\Gamma\left(\phi+1\right)}{\pi\left(g_{\mathrm{MPSK}}\right)^{\phi}} \int_0^{\pi-\frac{\pi}{M}} \left(\sin\theta\right)^{2\phi} d\theta. \tag{29}$$

We utilize the symmetry and periodicity of the sine function to rearrange the integration limits in (29) to obtain the more tractable form of

$$\int_0^{\pi-\frac{\pi}{M}} \left(\sin\theta\right)^{2\phi} d\theta = \int_0^{\frac{\pi}{2}} \left(\sin\theta\right)^{2\phi} d\theta + \int_{\frac{\pi}{M}}^{\frac{\pi}{2}} \left(\sin\theta\right)^{2\phi} d\theta. \tag{30}$$

Solving the integrals in (30) yields a new closed-form expression for the asymptotic SER of M-PSK given by

$$P_{s,\mathrm{MPSK}}^{\infty} = \left(G_{a,\mathrm{MPSK}}\overline{\gamma}_1\right)^{-G_{d,\mathrm{MPSK}}} + o\left(\overline{\gamma}_1^{-G_{d,\mathrm{MPSK}}}\right), \tag{31}$$

where the diversity order is

$$G_{d,\mathrm{MPSK}} = N_R \times \min\{N_S, N_D K\} \tag{32}$$

and the array gain is

$$G_{a,\mathrm{MPSK}} = \left[\frac{\delta\Gamma\left(\phi+\frac{1}{2}\right)}{2\sqrt{\pi}\left(g_{\mathrm{MPSK}}\right)^{\phi}} + \frac{\delta\Gamma\left(\phi+1\right)\sqrt{1-g_{\mathrm{MPSK}}}}{\pi\left(g_{\mathrm{MPSK}}\right)^{\phi}} \times {}_2F_1\left(\frac{1}{2}, \frac{1}{2}-\phi; \frac{3}{2}; 1-g_{\mathrm{MPSK}}\right)\right]^{-\frac{1}{\phi}}, \tag{33}$$

with ϕ and δ defined in (16) and (17), respectively.

Based on the new asymptotic expressions in (26) and (31), we next highlight the following two remarks.

Remark 1: Both M-QAM and M-PSK achieve the same diversity order of $N_R \times \min\{N_S, N_D K\}$, as indicated by (27) and (32). This implies that the quality of the first hop is characterized as $N_S N_R$ and the quality of the second hop is characterized as $N_R N_D K$. According to the diversity order, we confirm that the end-to-end network performance is dominated by the weaker hop.

Remark 2: For the same number of antennas, the performance gap between M-QAM and M-PSK is determined by their respective array gains in (28) and (33). As expected, we find that $G_{a,\mathrm{MQAM}} = G_{a,\mathrm{MPSK}}$ for $M = 4$. For higher order modulations, we find that for the same SER, M-QAM is superior to M-PSK by an SNR gap of $10\log\left(\frac{G_{a,\mathrm{MQAM}}}{G_{a,\mathrm{MPSK}}}\right)$ dB.

V. SER-Optimized Power Allocation

The transmit power is a key network resource affecting the lifetime and scalability in MIMO MRN. In this section, we address the following question: *"Given the proposed cascaded TAS/MRC that attains full diversity order, how to maximize network performance by optimally allocating transmit power without expending additional resources?"* To answer this question, we seek to identify the optimal power assignment at the source and the relay that minimizes the SER under a total transmit power constraint E_{T}. Let η denote the power assignment factor which determines the power assignment at the source and the relay such that $E_{\mathrm{S}} = \eta E_{\mathrm{T}}$ and $E_{\mathrm{R}} = (1-\eta)\,E_{\mathrm{T}}$. The average SNRs of the first and second hops can be re-expressed as $\overline{\gamma}_1 = \overline{\mathbf{h}}\eta E_{\mathrm{T}}/\Omega$ and $\overline{\gamma}_{2_k} = \overline{\mathbf{g}}\,(1-\eta)\,E_{\mathrm{T}}/\Omega$, respectively, where $\overline{\mathbf{h}} = \mathbb{E}\left[\|\mathbf{h}_{\mathrm{SR}}\|^2\right]$ and $\overline{\mathbf{g}} = \mathbb{E}\left[\|\mathbf{g}_{\mathrm{RD}_k}\|^2\right]$. Applying our SER solutions, we formulate the optimization problem as

$$\min_{\eta} \; P_s \quad \text{subject to} \quad 0 < \eta < 1. \tag{34}$$

Therefore, the optimal power assignment for M-QAM and M-PSK is the value of η that satisfies

$$\frac{\partial P_{s,\mathrm{MQAM}}}{\partial \eta} = 0 \tag{35}$$

and

$$\frac{\partial P_{s,\mathrm{MPSK}}}{\partial \eta} = 0, \tag{36}$$

respectively. We first focus on the approximate SER in (20) and (22). Taking the second derivative with respect to η, we find that $\partial^2 P_{s,\mathrm{MQAM}}/\partial^2\eta > 0$ and $\partial^2 P_{s,\mathrm{MPSK}}/\partial^2\eta > 0$ which confirm that $P_{s,\mathrm{MQAM}}$ and $P_{s,\mathrm{MPSK}}$ are convex functions of η. Therefore, substituting (20) into (35) for M-QAM and (22) into (36) for M-PSK, the optimal power assignment are solved using numerical root-finding [31].

To find a tractable closed-form solution for η, we turn our attention to the asymptotic SER in (26) and (31). Here, we jointly consider E_{S} and E_{R}.

1) M-QAM: Based on (26), the objective function for M-QAM is given by

$$P^{\infty}_{s,\mathrm{MQAM}_{\mathrm{OPA}}} = \left(\Phi\left(N_S N_R, \frac{1}{(N_R!)^{N_S}}\right)\frac{\overline{\mathbf{h}}\eta E_{\mathrm{T}}}{\Omega}\right)^{-N_S N_R} + \left(\Phi\left(N_R N_D K, \frac{1}{(N_D!)^{N_R K}}\right)\frac{\overline{\mathbf{g}}\,(1-\eta)\,E_{\mathrm{T}}}{\Omega}\right)^{-N_R N_D K}, \tag{37}$$

where $\Phi(\phi,\delta) = G_{a,\mathrm{MQAM}}$. Substituting (37) into (35) and applying some mathematical manipulations, the optimal power assignment is the value of η which satisfies

$$\frac{\eta^{N_S N_R+1}}{(1-\eta)^{N_R N_D K+1}} = \frac{N_S}{N_D K}\left(\frac{E_{\mathrm{T}}}{\Omega}\right)^{N_R(N_D K - N_S)} \times \frac{\left(\Phi\left(N_R N_D K, \frac{1}{(N_D!)^{N_R K}}\right)\overline{\mathbf{g}}\right)^{N_R N_D K}}{\left(\Phi\left(N_S N_R, \frac{1}{(N_R!)^{N_S}}\right)\overline{\mathbf{h}}\right)^{N_S N_R}}. \tag{38}$$

For the special case with $N_S = N_D K$, the optimal power assignment can be simplified as

$$\eta = \left(1 + \frac{(N_R!)^{\frac{N_S}{N_S N_R+1}}}{(N_D!)^{\frac{N_R K}{N_S N_R+1}}}\left(\frac{\overline{\mathbf{h}}}{\overline{\mathbf{g}}}\right)^{\frac{N_S N_R}{N_S N_R+1}}\right)^{-1}. \tag{39}$$

2) M-PSK: Based on (31), the objective function for M-PSK is given by

$$P^{\infty}_{s,\mathrm{MPSK}_{\mathrm{OPA}}} = \left(\Psi\left(N_S N_R, \frac{1}{(N_R!)^{N_S}}\right)\frac{\overline{\mathbf{h}}\eta E_{\mathrm{T}}}{\Omega}\right)^{-N_S N_R} + \left(\Psi\left(N_R N_D K, \frac{1}{(N_D!)^{N_R K}}\right)\frac{\overline{\mathbf{g}}\,(1-\eta)\,E_{\mathrm{T}}}{\Omega}\right)^{-N_R N_D K}, \tag{40}$$

where $\Psi(\phi,\delta) = G_{a,\mathrm{MPSK}}$. Substituting (40) into (36) and after some mathematical manipulations, the optimal power assignment is given by

$$\frac{\eta^{N_S N_R+1}}{(1-\eta)^{N_R N_D K+1}} = \frac{N_S}{N_D K}\left(\frac{E_{\mathrm{T}}}{\Omega}\right)^{N_R(N_D K - N_S)} \times \frac{\left(\Psi\left(N_R N_D K, \frac{1}{(N_D!)^{N_R K}}\right)\overline{\mathbf{g}}\right)^{N_R N_D K}}{\left(\Psi\left(N_S N_R, \frac{1}{(N_R!)^{N_S}}\right)\overline{\mathbf{h}}\right)^{N_S N_R}}. \tag{41}$$

For the special case with $N_S = N_D K$, the optimal power assignment is the same as that in (39).

VI. Numerical Results

We present numerical results to illustrate the impact of the number of antennas and destinations on the SER. In all the figures, the variance of the fading coefficients is normalized to unity, i.e., $\mathbb{E}\left[\|\mathbf{h}_{\mathrm{SR}}\|^2\right] = \mathbb{E}\left[\|\mathbf{g}_{\mathrm{RD}_k}\|^2\right] = 1$, and the PSD of the noise is normalized to unity, i.e., $\Omega = 1$. Throughout this section, the solid curves represent the exact SER from (19) and (21), the dashed curves represent the approximate SER from (20) and (22), and the dotted curves represent the asymptotic SER from (26) and (31). We use the '$+$' and '$\bullet$' symbols to mark Monte Carlo simulation points for CNB relaying with M-QAM and M-PSK, respectively. In all the figures, an excellent agreement between simulations and analysis is attested in the medium to high SNR regime. Moreover, our exact SER curves provide a tight approximation to the simulations in the low SNR regime.

Figs. 2 and 3 plot the SER for 64-QAM and 8-PSK, respectively. In these figures, we consider uniform power assignment with $E_{\mathrm{S}} = E_{\mathrm{R}}$ (or equivalently $\overline{\gamma}_1 = \overline{\gamma}_2$). We see that our approximate curves for both M-QAM and M-PSK are accurate representations of the exact SER. Furthermore,

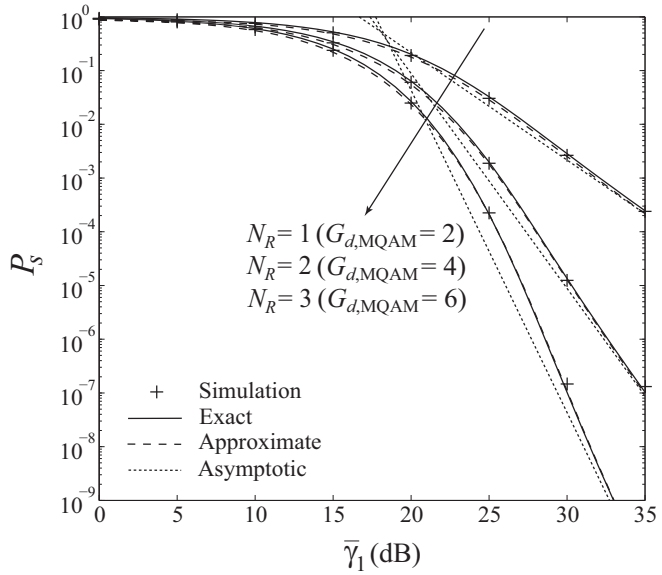

Fig. 2. SER for 64-QAM with $N_S = 2$, $N_D = 1$, and $K = 3$.

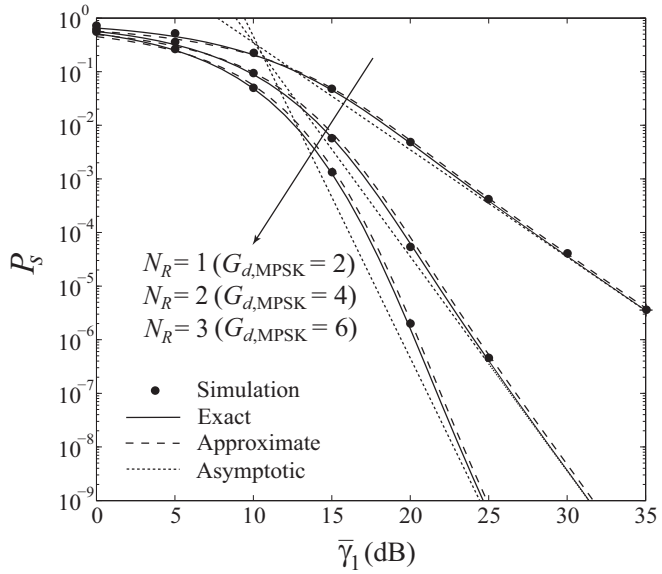

Fig. 3. SER for 8-PSK with $N_S = 2$, $N_D = 1$, and $K = 3$.

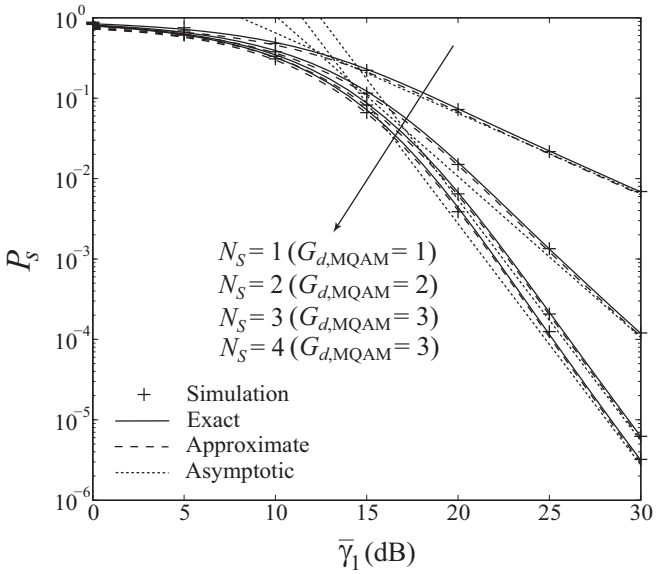

Fig. 4. SER for 16-QAM with $N_R = 1$, $N_D = 1$, and $K = 3$.

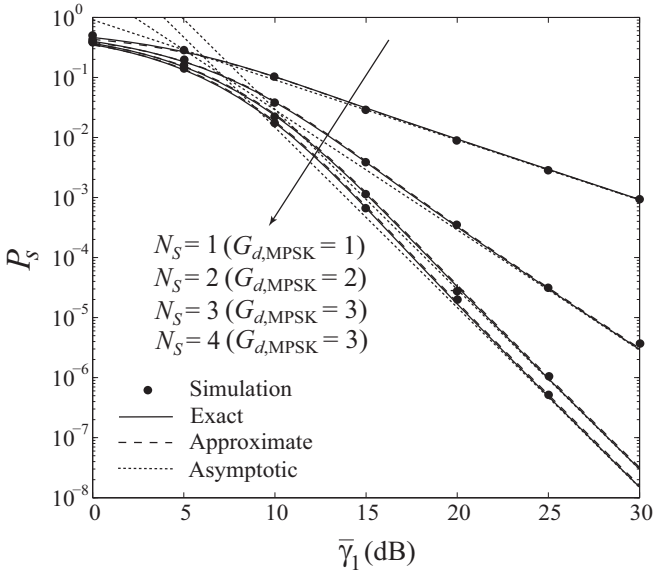

Fig. 5. SER for QPSK with $N_R = 1$, $N_D = 1$, and $K = 3$.

our asymptotic curves precisely predict the diversity order and the array gain. The figures demonstrate a pronounced decrease in the SER with increasing N_R. For example at $P_s = 10^{-3}$, increasing N_R from 1 to 2 results in an SNR advantage of 6.5 dB and 6 dB for 64-QAM and 8-PSK, respectively. This can be explained by the fact that the diversity order is directly proportional to N_R.

Figs. 4 and 5 plot the SER for 16-QAM and 4-PSK, respectively. The figures demonstrate the impact of N_S on the SER with uniform power assignment. For example at $P_s = 10^{-4}$, increasing N_S from 2 to 3 results in a prominent SNR advantage of 4 dB and 3.8 dB for 16-QAM and 4-PSK, respectively. This is due to the fact that the diversity order increases with N_S for $N_S < N_D K$. Increasing N_S from 3 to 4 offers a modest SNR advantage of 0.8 dB and 0.7 dB for 16-QAM and 4-PSK, respectively. This advantage lies solely in the array gain since the diversity order indicated by the parallel slopes of the asymptotes remains unchanged. Indeed, the figures confirm that the diversity order is limited by the minimum of N_S and $N_D K$.

Fig. 6 plots the SER versus K for 16-QAM and 16-PSK. The figure demonstrates the impact of K on the SER with $\overline{\gamma}_1 = \overline{\gamma}_2 = 30$ dB. We observe a prominent decrease in the SER as K increases from 1 to 4. For example, increasing K from 1 to 2 brings a SER reduction of 60-fold for 16-QAM and 25-fold for 16-PSK. This is due to an increase in the diversity order for $N_D K < N_S$. Further increasing K from 4 to 8 yields a marginal improvement since the diversity order remains unchanged.

Fig. 7 plots the SER versus η for 16-QAM. The figure re-

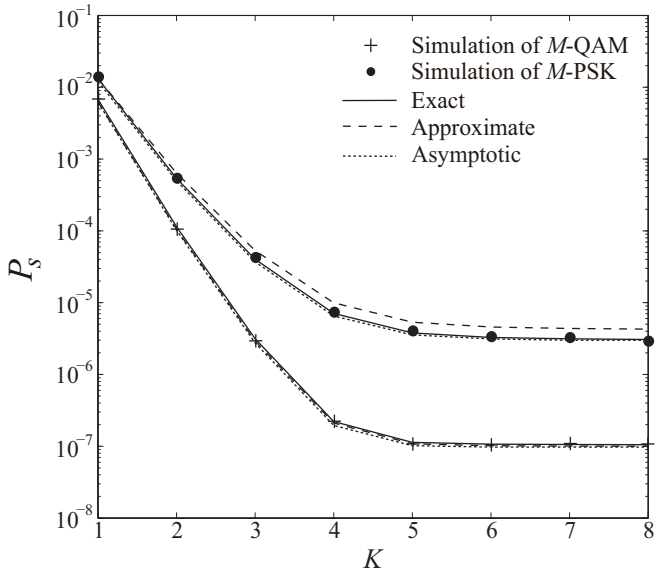

Fig. 6. SER for 16-QAM and 16-PSK with $N_S = 4$, $N_R = 1$, and $N_D = 1$.

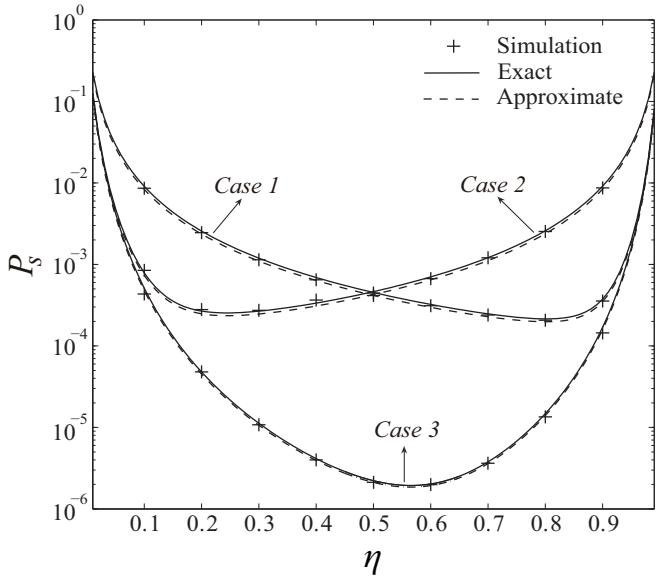

Fig. 7. SER for 16-QAM with three cases.

veals the optimal power assignment at the source and the relay to minimize the SER. Allocating the total power between the source and the relay is a key design choice towards network sustainability – reducing the overall power consumption and related energy costs. We set $E_{\mathrm{T}}/\Omega = 30$ dB and consider the following three cases based on the relationship of N_S and $N_D K$.

1) *Case 1*: $(N_S, N_R, N_D, K) = (2, 1, 2, 2)$. In this case, we consider $N_S < N_D K$. We observe that the SER is minimized at $\eta = 0.80$. This means that the optimal power assignment is achieved by allocating 80% of the total power to the source and 20% to the relay. Recall that $\eta = 0.5$ represents uniform power assignment. As such, we see that our optimal power assignment yields a superior performance compared to uniform power assignment.
2) *Case 2*: $(N_S, N_R, N_D, K) = (4, 1, 1, 2)$. In this case, we consider $N_S > N_D K$. The figure shows that the SER is minimized at $\eta = 0.25$.
3) *Case 3*: $(N_S, N_R, N_D, K) = (4, 1, 2, 2)$. In this case, we consider $N_S = N_D K$. We observe that the SER is minimized at $\eta = 0.57$.

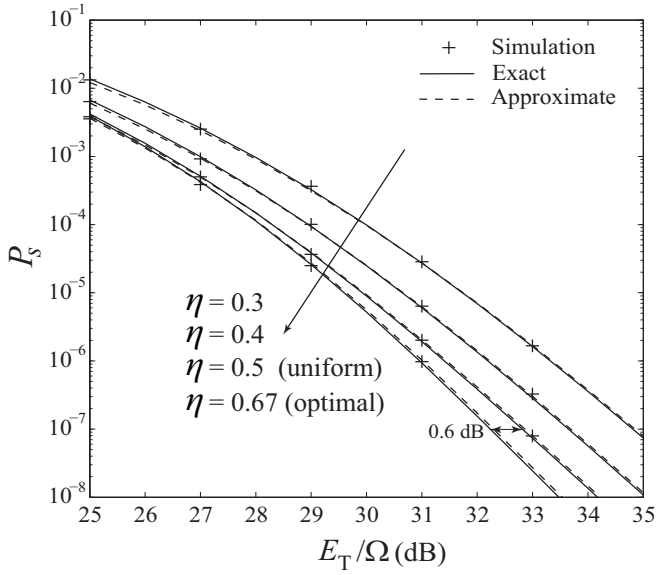

Fig. 8. SER for 64-QAM with $N_S = 8$, $N_R = 1$, $N_D = 4$, and $K = 2$.

We confirm that the optimal η in each of the three cases shown in Fig. 7 is in precise agreement with the asymptotic-based solution in (38).

Fig. 8 plots the SER versus E_{T}/Ω for 64-QAM. The figure demonstrates the benefits of the optimal power assignment for $N_S = N_D K$ in (39). In this figure, we consider the case of $(N_S, N_R, N_D, K) = (8, 1, 4, 2)$. In this case, the optimal power assignment is calculated from (39) as $\eta = 0.67$. This figure clearly indicates that the optimal power assignment guarantees a lower SER than the other values of η. For example at $P_s = 10^{-7}$, the optimal power assignment (i.e., $\eta = 0.67$) brings an SNR advantage of 0.6 dB over the uniform power assignment (i.e., $\eta = 0.5$).

VII. Conclusion

We proposed and analyzed cascaded TAS/MRC in MIMO MRN with N_S, N_R, and N_D antennas at the source, relay, and each of the K destinations, respectively. Important quality of service measures were provided based on our new exact closed-form expressions for the CDF, PDF, and MGF of the instantaneous end-to-end SNR. We further derived a new accurate approximation for the SER under M-QAM. The asymptotic SER for M-QAM and M-PSK were presented which clearly indicate the diversity order and the array gain. Based on our approximate and asymptotic SER expressions, optimal power assignment that minimize the SER was evaluated.

APPENDIX A
PROOF OF THEOREM 1

In TAS/MRC, the CDF and PDF of the instantaneous per-hop SNRs $Z = \{\gamma_1, \gamma_{2_k}\}$ are given by [17]

$$F_Z(\gamma) = \left(1 - e^{-\frac{\gamma}{\overline{\gamma}_i}} \sum_{m=1}^{N_q} \frac{(\gamma/\overline{\gamma}_i)^{m-1}}{(m-1)!}\right)^{N_p} \tag{42}$$

and

$$f_Z(\gamma) = \frac{N_p \gamma^{N_q-1} e^{-\frac{\gamma}{\overline{\gamma}_i}}}{\overline{\gamma}_i^{N_q}(N_q-1)!} \left(1 - e^{-\frac{\gamma}{\overline{\gamma}_i}} \sum_{m=1}^{N_q} \frac{(\gamma/\overline{\gamma}_i)^{m-1}}{(m-1)!}\right)^{N_p-1}, \tag{43}$$

respectively, where $(N_p, N_q, i) \in \{(N_S, N_R, 1), (N_R, N_D, 2)\}$. Assuming that the first hop and the second hop are subject to independent Rayleigh fading, the CDF of the highest instantaneous end-to-end SNR is obtained as

$$\begin{aligned} F_{\gamma_s}(\gamma) &= \int_0^\infty \Pr\left[\frac{\gamma_1\gamma_{2_k}}{\gamma_1+\gamma_{2_k}+\xi} \le \gamma|\gamma_1\right]^K f_{\gamma_1}(\gamma_1)\, d\gamma_1 \\ &= \int_0^\gamma \Pr\left[\gamma_{2_k} > \frac{\gamma_1\gamma}{\gamma_1-\gamma}|\gamma_1\right]^K f_{\gamma_1}(\gamma_1)\, d\gamma_1 \\ &\quad + \int_\gamma^\infty \Pr\left[\gamma_{2_k} \le \frac{\gamma_1\gamma}{\gamma_1-\gamma}|\gamma_1\right]^K f_{\gamma_1}(\gamma_1)\, d\gamma_1 \\ &= \underbrace{\int_0^\gamma f_{\gamma_1}(\gamma_1)\, d\gamma_1}_{\ell_1} \\ &\quad + \underbrace{\int_\gamma^\infty \left[F_{\gamma_{2_k}}\left(\frac{\gamma(\gamma_1+\xi)}{\gamma_1-\gamma}\right)\right]^K f_{\gamma_1}(\gamma_1)\, d\gamma_1}_{\ell_2}, \end{aligned} \tag{44}$$

where $\Pr[\cdot]$ denotes probability. Substituting (42) and (43) into (44) and applying the binomial expansion given in [32, eq. (1.111)], ℓ_2 can be derived as

$$\begin{aligned} \ell_2 = \int_\gamma^\infty f_{\gamma_1}(\gamma_1)\, d\gamma_1 + \frac{N_S}{\Gamma(N_R)\overline{\gamma}_1^{N_R}} \sum_{\kappa=1}^{N_RK} \binom{N_RK}{\kappa} (-1)^\kappa \\ \times \sum_{\lambda=0}^{N_S-1} \binom{N_S-1}{\lambda} (-1)^\lambda \ell_3, \end{aligned} \tag{45}$$

where

$$\begin{aligned} \ell_3 = \int_\gamma^\infty \gamma_1^{N_R-1} e^{-\frac{\kappa\gamma(\gamma_1+\xi)}{\overline{\gamma}_2(\gamma_1-\gamma)} - \frac{(\lambda+1)\gamma_1}{\overline{\gamma}_1}} \\ \times \left(\sum_{\iota=1}^{N_D} \frac{\left(\frac{\gamma(\gamma_1+\xi)}{\overline{\gamma}_2(\gamma_1-\gamma)}\right)^{\iota-1}}{(\iota-1)!}\right)^\kappa \left(\sum_{\mu=1}^{N_R} \frac{\left(\frac{\gamma_1}{\overline{\gamma}_1}\right)^{\mu-1}}{(\mu-1)!}\right)^\lambda d\gamma_1. \end{aligned} \tag{46}$$

Then we set $\gamma_1 = x + \gamma$ into (46). Applying [33, eq. (9)] to expand the power of polynomial in (46) and utilizing [32, eq.(3.471.9)] to solve the resultant integral, we obtain the desired result in (10), thus completing the proof.

APPENDIX B
PROOF OF THEOREM 3

We first derive the first non-zero order expansion of $F_{\gamma_s}(\gamma)$. By defining $\overline{\gamma}_2 = \omega\overline{\gamma}_1$ and $\gamma = \chi\overline{\gamma}_1$ in (10), we re-express $F_{\gamma_s}(\gamma)$ as a function of χ, $F(\chi)$, which is given by

$$\begin{aligned} F(\chi) =& 1 + \frac{2N_S}{\Gamma(N_R)} \sum_{\kappa=1}^{N_RK} \binom{N_RK}{\kappa} \sum_{\lambda=0}^{N_S-1} \binom{N_S-1}{\lambda} (-1)^{\kappa+\lambda} \\ &\times \sum_{\epsilon=0}^{N_R-1} \binom{N_R-1}{\epsilon} \prod_{v=1}^{N_D-1} \left[\sum_{j_v=0}^{j_{v-1}} \binom{j_{v-1}}{j_v} \left(\frac{1}{v!}\right)^{j_v-j_{v+1}}\right] \\ &\times \prod_{w=1}^{N_R-1} \left[\sum_{k_w=0}^{k_{w-1}} \binom{k_{w-1}}{k_w} \left(\frac{1}{w!}\right)^{k_w-k_{w+1}}\right] \sum_{\alpha=0}^{\psi_v} \binom{\psi_v}{\alpha} \\ &\times \sum_{\beta=0}^{\psi_w} \binom{\psi_w}{\beta} \left(\frac{\kappa}{\lambda+1}\right)^{\frac{\nu}{2}} \frac{\chi^{N_R+\psi_w+\psi_v}}{\omega^{\frac{\nu}{2}+\psi_v}} e^{-\chi\left(\lambda+1+\frac{\kappa}{\omega}\right)} \\ &\times K_\nu\left(2\chi\sqrt{\frac{\kappa(\lambda+1)}{\omega}}\right), \end{aligned} \tag{47}$$

where $\nu = N_R - \epsilon - \alpha + \psi_w - \beta$. By comparing (10) and (47) we find that the behavior of $F_{\gamma_s}(\gamma)$ at high SNRs is equivalent to the behavior of $F(\chi)$ around the origin. Applying the Taylor series expansion of the exponential function from [32, eq. (1.211.1)] and the Bessel function from [32, eq. (8.446)], we seek the first non-zero order of $F(\chi)$ and discard the higher order terms. Specifically, the first non-zero order of $F(\chi)$ can be studied based on three cases.

Case 1: $N_S < N_DK$. In this case, we obtain

$$F(\chi) = \frac{\chi^{N_SN_R}}{(N_R!)^{N_S}} + o\left(\chi^{N_SN_R}\right). \tag{48}$$

Case 2: $N_S > N_DK$. In this case, we obtain

$$F(\chi) = \frac{\chi^{N_RN_DK}}{(N_D!)^{N_RK}\,\omega^{N_RN_DK}} + o\left(\chi^{N_RN_DK}\right), \tag{49}$$

where $\omega = \overline{\gamma}_2/\overline{\gamma}_1$.

Case 3: $N_S = N_DK$. In this case, we obtain

$$\begin{aligned} F(\chi) = \left(\frac{1}{(N_R!)^{N_S}} + \frac{1}{(N_D!)^{N_RK}\,\omega^{N_RN_DK}}\right) \chi^{N_SN_R} \\ + o\left(\chi^{N_SN_R}\right). \end{aligned} \tag{50}$$

By substituting $\chi = \gamma/\overline{\gamma}_1$ into (48), (49) and (50), and summarizing the three cases above, the first non-zero order expansion of $F_{\gamma_s}(\gamma)$ in (14) is obtained. Next, we substitute (14) into (12), which results in the first non-zero order expansion of $M_{\gamma_s}(s)$.

APPENDIX C
PROOF OF EQUATION (20)

Recall that the MGF of γ_s is given by $M_{\gamma_s}(s) = \mathbb{E}_{\gamma_s}[\exp(s\gamma)]$. As such, we re-express $P_{s,\mathrm{MQAM}}$ as

$$\begin{aligned} P_{s,\mathrm{MQAM}} = \mathbb{E}_{\gamma_s}\left[\frac{4\Delta}{\pi}\int_0^{\frac{\pi}{2}} \exp\left(-\frac{g_{\mathrm{MQAM}}}{\sin^2\theta}\gamma\right) d\theta \right. \\ \left. -\frac{4\Delta^2}{\pi}\int_0^{\frac{\pi}{4}} \exp\left(-\frac{g_{\mathrm{MQAM}}}{\sin^2\theta}\gamma\right) d\theta\right]. \end{aligned} \tag{51}$$

Since the right-hand integral in (51) can be rewritten as

$$\int_0^{\frac{\pi}{4}} \exp\left(-\frac{g_{\mathrm{MQAM}}}{\sin^2\theta}\gamma\right) d\theta = \int_0^{\frac{\pi}{2}} \exp\left(-\frac{g_{\mathrm{MQAM}}}{\sin^2\theta}\gamma\right) d\theta - \int_{\frac{\pi}{4}}^{\frac{\pi}{2}} \exp\left(-\frac{g_{\mathrm{MQAM}}}{\sin^2\theta}\gamma\right) d\theta, \tag{52}$$

we can further re-express (51) as

$$P_{s,\mathrm{MQAM}} = \mathbb{E}_{\gamma_s}\left[\frac{4\Delta\left(1-\Delta\right)}{\pi}\underbrace{\int_0^{\frac{\pi}{2}} \exp\left(-\frac{g_{\mathrm{MQAM}}}{\sin^2\theta}\gamma\right) d\theta}_{\mathcal{I}_1} + \frac{4\Delta^2}{\pi}\underbrace{\int_{\frac{\pi}{4}}^{\frac{\pi}{2}} \exp\left(-\frac{g_{\mathrm{MQAM}}}{\sin^2\theta}\gamma\right) d\theta}_{\mathcal{I}_2}\right]. \tag{53}$$

Applying the formulae in [34], the integral $\mathcal{I}_1$ in (53) can be solved as

$$\frac{2}{\pi}\int_0^{\frac{\pi}{2}} \exp\left(-\frac{g_{\mathrm{MQAM}}}{\sin^2\theta}\gamma\right) d\theta \approx \frac{1}{6}\exp\left(-g_{\mathrm{MQAM}}\gamma\right) + \frac{1}{2}\exp\left(-\frac{4}{3}g_{\mathrm{MQAM}}\gamma\right). \tag{54}$$

Next, we approximate $\mathcal{I}_2$ in (53) with the area of trapezoid formula given by

$$\frac{1}{\pi}\int_{\frac{\pi}{4}}^{\frac{\pi}{2}} \exp\left(-\frac{g_{\mathrm{MQAM}}}{\sin^2\theta}\gamma\right) d\theta \approx \frac{1}{4}\exp\left(-g_{\mathrm{MQAM}}\gamma\right) + \frac{1}{4}\exp\left(-2g_{\mathrm{MQAM}}\gamma\right). \tag{55}$$

Finally, substituting (54) and (55) into (53) gives the desired result in (20).

REFERENCES

[1] J. N. Laneman, D. N. C. Tse, and G. W. Wornell, "Cooperative diversity in wireless networks: efficient protocols and outage behavior," *IEEE Trans. Inf. Theory*, vol. 50, no. 12, pp. 3062–3080, Dec. 2004.

[2] J. Sydir and R. Taori, "An evolved cellular system architecture incorporating relay stations," *IEEE Commun. Mag.*, vol. 47, no. 6, pp. 115–121, June 2009.

[3] S. W. Peters and R. W. Heath, "The future of WiMAX: multihop relaying with IEEE 802.16j," *IEEE Commun. Mag.*, vol. 47, no. 1, pp. 104–111, Jan. 2009.

[4] G. R. Hiertz, D. Denteneer, S. Max, R. Taori, J. Cardona, L. Berlemann, and B. Walke, "IEEE 802.11s: the WLAN mesh standard," *IEEE Wireless Commun.*, vol. 17, no. 1, pp. 104–111, Feb. 2010.

[5] J.-B. Kim and D. Kim, "Comparison of two SNR-based feedback schemes in multiuser dual-hop amplify-and-forward relaying networks," *IEEE Commun. Lett.*, vol. 12, no. 8, pp. 557–559, Aug. 2008.

[6] C. K. Sung and I. B. Collings, "Cooperative multiplexing with interference suppression in multiuser wireless relay networks," *IEEE Trans. Wireless Commun.*, vol. 9, no. 8, pp. 2528–2538, Aug. 2010.

[7] N. Yang, M. Elkashlan, and J. Yuan, "Outage probability of multiuser relay networks in Nakagami-m fading channels," *IEEE Trans. Veh. Technol.*, vol. 59, no. 5, pp. 2120–2132, June 2010.

[8] N. Yang, M. Elkashlan, and J. Yuan, "Impact of opportunistic scheduling on cooperative dual-hop relay networks," *IEEE Trans. Commun.*, vol. 59, no. 3, pp. 689–694, Mar. 2011.

[9] E. Telatar, "Capacity of multi-antenna Gaussian channels," *Europ. Trans. Telecommun.*, vol. 10, no. 6, pp. 585–595, Nov. 1999.

[10] G. J. Foschini, "Layered space-time architecture for wireless communications in a fading environment when using multiple antennas," *Bell Lab. Tech. J.*, vol. 6, no. 2, pp. 41–59, 1996.

[11] G. J. Foschini and M. J. Gans, "On limits of wireless communications in a fading environment when using multiple antennas," *Wireless Personal Commun.*, vol. 6, pp. 311–335, Mar. 1998.

[12] C.-B. Chae, T. Tang, R. W. Heath, and S. Cho, "MIMO relaying with linear processing for multiuser transmission in fixed relay networks," *IEEE Trans. Signal Process.*, vol. 56, no. 2, pp. 727–738, Feb. 2008.

[13] C.-H. Lee, J.-H. Lee, Y.-W. Kwak, Y.-H. Kim, and S.-C. Kim, "The realization of full duplex relay and sum rate analysis in multiuser MIMO relay channel," in *Proc. 2010 IEEE VTC – Fall*, pp. 1–5.

[14] Y. Yu and Y. Hua, "Power allocation for a MIMO relay system with multiple-antenna users," *IEEE Trans. Signal Process.*, vol. 58, no. 5, pp. 2823–2835, Mar. 2010.

[15] R. Zhang, C. C. Chai, and Y.-C. Liang, "Joint beamforming and power control for multiantenna relay broadcast channel with QoS constraints," *IEEE Trans. Signal Process.*, vol. 57, no. 2, pp. 726–737, Feb. 2009.

[16] Z. Chen, "Asymptotic performance of transmit antenna selection with maximal-ratio combining for generalized selection criterion," *IEEE Commun. Lett.*, vol. 8, no. 4, pp. 247–249, Apr. 2004.

[17] Z. Chen, J. Yuan, and B. Vucetic, "Analysis of transmit antenna selection/maximal ratio combining in Rayleigh fading channels," *IEEE Trans. Veh. Technol.*, vol. 54, no. 4, pp. 1312–1321, July 2005.

[18] P. L. Yeoh, M. Elkashlan, and I. B. Collings, "Exact and asymptotic SER of distributed TAS/MRC in MIMO relay networks," *IEEE Trans. Wireless Commun.*, vol. 10, no. 3, pp. 751–756, Mar. 2011.

[19] S. Thoen, L. Van der Perre, B. Gyselinckx, and M. Engels, "Performance analysis of combined transmit-SC/receive-MRC," *IEEE Trans. Commun.*, vol. 49, no. 1, pp. 5–8, Jan. 2001.

[20] L. Yang and M.-S. Alouini, "Performance analysis of multiuser selection diversity," *IEEE Trans. Veh. Technol.*, vol. 55, no. 6, pp. 1848–1861, Nov. 2006.

[21] H. Holma and A. Toskala, *HSDPA/HSUPA for UMTS: High Speed Radio Access for Mobile Communications*. John Wiley and Sons, 2006.

[22] V. Vanghi, A. Damnjanovic, and B. Vojcic, *The CDMA2000 System for Mobile Communications: 3G Wireless Evolution*. Prentice Hall, 2004.

[23] R. H. Y. Louie, Y. Li, H. Suraweera, and B. Vucetic, "Performance analysis of beamforming in two hop amplify and forward relay networks with antenna correlation," *IEEE Trans. Wireless Commun.*, vol. 8, no. 6, pp. 3132–3141, June 2009.

[24] T. Q. Duong, G. C. Alexandropoulos, H.-J. Zepernick, and T. A. Tsiftsis, "Orthogonal space-time block codes with CSI-assisted amplify-and-forward relaying in correlated Nakagami-m fading channels," *IEEE Trans. Veh. Technol.*, vol. 60, no. 3, pp. 882–889, Mar. 2011.

[25] N. S. Ferdinand and N. Rajatheva, "Unified performance analysis of two-hop amplify-and-forward relay systems with antenna correlation," *IEEE Trans. Wireless Commun.*, vol. 10, no. 5, pp. 3002–3011, Sep. 2011.

[26] J. Yang, P. Fan, T. Q. Duong, and X. Lei, "Exact performance of two-way AF relaying in Nakagami-m fading environment," *IEEE Trans. Wireless Commun.*, vol. 10, no. 3, pp. 980–987, Mar. 2011.

[27] A. P. Prudinikov, Y. A. Brychkov, and O. I. Marichev, *Integrals and Series, Vol. 2*. Gordon and Breach Science Publishers, 1986.

[28] M. K. Simon and M.-S. Alouini, *Digital Communication over Fading Channels: A Unified Approach to Performance Analysis*. John Wiley and Sons, 2000.

[29] M. R. McKay, A. Zanella, I. B. Collings, and M. Chiani, "Error probability and SINR analysis of optimum combining in Rician fading," *IEEE Trans. Commun.*, vol. 57, no. 3, pp. 676–687, Mar. 2009.

[30] Z. Wang and G. B. Giannakis, "A simple and general parameterization quantifying performance in fading channels," *IEEE Trans. Commun.*, vol. 51, no. 8, pp. 1389–1398, Aug. 2003.

[31] S. Boyd and L. Vandenberghe, *Convex Optimization*. Cambridge University Press, 2004.

[32] I. S. Gradshteyn and I. M. Ryzhik, *Table of Integrals, Series and Products*, 7th edition. Academic Press, 2007.

[33] S. Choi and Y.-C. Ko, "Performance of selection MIMO systems with generalized selection criterion over Nakagami-m fading channels," *IEICE Trans. Commun.*, vol. E89-B, no. 12, pp. 3467–3470, Dec. 2006.

[34] M. Chiani, D. Dardari, and M. K. Simon, "New exponential bounds and approximations for the computation of error probability in fading channels," *IEEE Trans. Wireless Commun.*, vol. 2, no. 4, pp. 840–845, July 2003.

Nan Yang (S'09-M'11) received the B.S. degree in Electronics from China Agricultural University, China, in 2005, the M.S. degree in Electronic Engineering from Beijing Institute of Technology, China in 2007, and the Ph.D. degree in Electronic Engineering from Beijing Institute of Technology, China, in 2010. From 2008 to 2010, he was a visiting Ph.D. student with the School of Electrical Engineering and Telecommunications at the University of New South Wales, Australia. In 2010, he joined the Wireless and Networking Technologies Laboratory at the Commonwealth Scientific and Industrial Research Organization (CSIRO), Australia. He is also holding a visiting appointment at the University of New South Wales, Australia. His general research interests lie in the area of communications theory and signal processing, with specific interests in cooperative communications, MIMO systems, resource allocation, and physical layer security.

Phee Lep Yeoh (S'08-M'12) received the B.E. degree with University Medal from the University of Sydney, Australia, in 2004, and the Ph.D. degree from the University of Sydney, Australia, in 2012. From 2004 to 2008, he worked in the wireless engineering division at Telstra Australia as radio network design and optimization engineer. From 2008 to 2012, he was with the Telecommunications Laboratory at the University of Sydney and the Wireless and Networking Technologies Laboratory at the Commonwealth Scientific and Industrial Research Organization (CSIRO), Sydney, Australia. In 2012, he joined the Department of Electrical and Electronic Engineering at the University of Melbourne, Australia. He was a recipient of the University of Sydney Postgraduate Award, the Norman I Price Scholarship, and the CSIRO Postgraduate Scholarship. His research interests include cooperative communications, MIMO, cross-layer optimization, and physical layer security.

Maged Elkashlan (M'06) received the Ph.D. degree in Electrical Engineering from the University of British Columbia, Canada, in 2006. From 2006 to 2007, he was with the Laboratory for Advanced Networking at the University of British Columbia. From 2007 to 2011, he was with the Wireless and Networking Technologies Laboratory at the Commonwealth Scientific and Industrial Research Organization (CSIRO), Australia. He has also held adjunct appointment at the University of Technology Sydney, Australia, between 2008 and 2011. In 2011, he joined the School of Electronic Engineering and Computer Science at Queen Mary, University of London, United Kingdom. He also holds visiting faculty appointments at the University of New South Wales, Australia and Beijing University of Posts and Telecommunications, China. His research interests include distributed wireless networks, cooperative wireless networks, MIMO systems, cognitive radio, and physical layer security. He has served as Technical Program Committee member for several IEEE conferences such as IEEE International Conference on Communications (ICC) and IEEE Global Communications Conference (GLOBECOM).

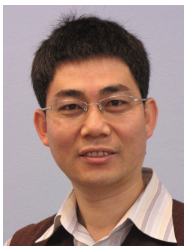

Jinhong Yuan (M'02-SM'11) received the B.E. and Ph.D. degrees in electronics engineering from Beijing Institute of Technology, Beijing, China, in 1991 and 1997, respectively. From 1997 to 1999 he was a Research Fellow at the School of Electrical Engineering, the University of Sydney, Sydney, Australia. In 2000 he joined the School of Electrical Engineering and Telecommunications, the University of New South Wales, Sydney, Australia, where he is currently a Professor for Telecommunications of the school. He has published two books, two book chapters, over 190 papers in telecommunications journals and conference proceedings and 40 industrial reports. He is a co-inventor of one patent on MIMO systems and two patents on low-density-parity-check (LDPC) codes. He co-authored three Best Paper Awards and one Best Poster Award, including a Best Paper Award of IEEE Wireless Communications and Networking Conference (WCNC), Cancun, Mexico in 2011, and a Best Paper Award of IEEE International Symposium on Wireless Communications Systems (ISWCS), Trondheim, Norway in 2007. His publications are available from http://www2.ee.unsw.edu.au/wcl/JYuan.html. He serves as the IEEE NSW Chair of joint Communications/Signal Processions/Ocean Engineering Chapter. His current research interests include error control coding and information theory, communication theory, and wireless communications.

Iain B. Collings (S'92-M'95-SM'02) received the B.E. degree in Electrical and Electronic Engineering from the University of Melbourne in 1992, and the Ph.D. degree in Systems Engineering from the Australian National University in 1995. Currently he is the Research Director of the Wireless and Networking Technologies Laboratory, and one of the CEOs Science Leaders, at the Australian Commonwealth Scientific and Industrial Research Organisation (CSIRO). Prior to this he was an Associate Professor at the University of Sydney (1999-2005); a Lecturer at the University of Melbourne (1996-1999); and a Research Fellow in the Australian Cooperative Research Centre for Sensor Signal and Information Processing (1995). He has published over 200 research papers in the area of mobile digital communications. More specifically, adaptive multi-carrier modulation, multi-user and MIMO systems, and ad hoc and sensor networks. In 2009 he was awarded the Engineers Australia IREE Neville Thiele Award for outstanding achievements in engineering and in 2011 he was awarded the Stephen O. Rice Prize from the IEEE TRANSACTIONS ON COMMUNICATIONS.

Dr. Collings served as an Editor for the IEEE TRANSACTIONS ON WIRELESS COMMUNICATIONS (2002-2009), and for the *Elsevier Physical Communication Journal* (PHYCOM) (since 2007). He has served as a Co-Chair of the Technical Program Committee for IEEE International Conference on Communications (ICC) 2013 and IEEE Vehicular Technology Conf. (VTC) Spring 2011; and as a Vice Chair of the TPC for IEEE Wireless Communications and Networking Conference (WCNC) 2010 and IEEE VTC Spring 2006; as well as serving on a number of other TPCs and organizing committees of IEEE conferences. He is a founding organizer of the Australian Communication Theory Workshops 2000–11. He also served as the Chair of the Joint Communications & Signal Processing Chapter in the IEEE NSW Section (2008–2010), as well as serving as the Secretary of the IEEE NSW Section (2010).